

## Mechanochemical Synthesis and Characterisation of Bismuth-Niobium Oxide Ion Conductors

S.N. Ng\*, Y.P. Tan\* and Y.H. Taufiq-Yap

Department of Chemistry, Faculty of Science, Universiti Putra Malaysia,  
43400 UPM Serdang, Selangor, Malaysia

\* Corresponding authors: sinnee83@gmail.com, yptan@fsas.upm.edu.my

**Abstract:** *Bismuth niobate solid solutions,  $Bi_xNbO_5$  ( $2.5 \leq x \leq 6$ ), have been prepared using a mechanochemical method. The solid solutions were also prepared using a solid-state conventional method for comparison purposes.  $Bi_3NbO_7$  was successfully obtained via a mechanochemical method at a lower synthesis temperature (milled at 1000 rpm for one hour followed by heating at 700°C for 24 h) than the conventional solid-state method. Electrical properties of the single-phase materials were studied by AC impedance spectroscopy. Further characterization of the materials was carried out using differential thermal analysis (DTA) and thermogravimetric analysis (TGA). The results showed that no thermal changes and phase transitions were observed and all materials were thermally stable.*

**Keywords:** bismuth niobate, mechanochemical, solid-state reaction, impedance spectroscopy

### 1. INTRODUCTION

Ionic conductors have provided a fascinating interdisciplinary field of study for over a century. In oxygen ion conductors, current flow occurs by the movement of an oxide ion through the crystal lattice. As well as the intrinsic interest in these materials, there has been a continued drive for their applications in technological devices such as solid oxide fuel cells (SOFCs), oxygen sensors, and many other applications. These entire devices offer the potential of enormous commercial and ecological benefits provided suitable high performance materials can be developed.<sup>1-4</sup> Yttria-stabilized zirconia (YSZ), which is used as the electrolyte in SOFC operates at a temperature around 1000°C. Thus, high operating temperatures will result in high fabrication costs and also affect the material stability and compatibility and the thermal degradation of the electrolyte itself. Therefore, there is a continuing effort to search for oxide ion conductors that can operate at lower temperature in order to reduce costs.

Bismuth oxide,  $\text{Bi}_2\text{O}_3$ , is recognized as a good oxide ion conductor due to its crystal structure (fluorite type) and its high ratio of oxygen vacancies.  $\text{Bi}_2\text{O}_3$  exists in four polymorphs, which are  $\alpha$ ,  $\beta$ ,  $\gamma$ , and  $\delta$ . The high-temperature form of bismuth oxide,  $\delta\text{-Bi}_2\text{O}_3$ , which has an oxygen-deficient fluorite-type structure, has been recognized as one of the best solid-state oxide ion conductors due to the high concentration of intrinsic oxygen vacancies.<sup>5</sup> However,  $\delta\text{-Bi}_2\text{O}_3$  is only stable in a narrow temperature range from 730°C to its melting point at 824°C. Below 730°C, the monoclinic  $\alpha\text{-Bi}_2\text{O}_3$  is the stable phase. In order to enhance the stability of the high-temperature and highly conducting  $\delta$ -phase, it can be doped with transition metal oxides such as  $\text{Nb}_2\text{O}_5$ ,  $\text{Ta}_2\text{O}_5$ ,  $\text{WO}_3$  or rare-earth oxides.<sup>6-9</sup> Among the many choices of substituting cations in  $\delta\text{-Bi}_2\text{O}_3$ ,  $\text{Nb}^{5+}$  is probably the most frequently used due to its high efficiency in stabilizing the cubic phase at room temperature.<sup>10</sup>

Bismuth niobate ( $\text{Bi}_3\text{NbO}_7$ ) exists in two crystallographic configurations, a tetragonal (type III) phase and a pseudocubic (type II) phase. The tetragonal phase shows a higher electrical conductivity than the pseudocubic phase. It was suggested that this is associated with the redistribution of the oxygen sublattice (or oxygen vacancies) induced by superstructure ordering in tetragonal  $\text{Bi}_3\text{NbO}_7$ , which appears to increase the mobility of free charge carriers and therefore improves the electrical conductivity. The plots of ionic conductivity versus reciprocal temperature are adequately fitted by the Arrhenius law:  $\sigma_T = \sigma_0 \exp(-E_a/KT)$ . The activation energies ( $E_a$ ) of oxygen ion diffusion for the Type II phase was higher than the Type III phase. The lower diffusion activation energy of the tetragonal phase shows that the Type III  $\text{Bi}_3\text{NbO}_7$  structure offers a lower energy barrier to oxide ion migration than the Type II phase. Over the entire temperature range, the tetragonal phase exhibits a higher electrical conductivity than that of the cubic phase.<sup>10-11</sup> In this paper, we examine the properties of the solid solutions in  $\text{Bi}_3\text{NbO}_7$  (type III), which include the phase purity, thermal stability, and the electrical properties.

Preparation via a traditional solid-state reaction usually requires high temperatures and long firing cycles leading to the inevitable coarsening of particles and aggregation of the powders, which results in poor microstructures and properties of electroceramics. The mechanochemical process, which is also known as mechanical alloying, has been recently employed to prepare oxides and compounds with smaller particle sizes. This technique is superior to both the conventional solid-state method and wet chemistry-based processing routes for several reasons. This method can provide better chemical mixing and produce materials with smaller particle sizes, thus enhancing the electrical properties of the materials. Furthermore, the mechanochemical method may produce single-phase materials at lower temperatures and shorten the synthesis time.<sup>12-13</sup>

## 2. EXPERIMENTAL

Solid solutions of  $\text{Bi}_x\text{Nb}_1\text{O}_6$  ( $2.5 \leq x \leq 7$ ) were synthesized using a mechanochemical and a conventional solid-state method. For the mechanochemical method, the stoichiometric mixtures of  $\text{Bi}_2\text{O}_3$  (99.9% Aldrich) and  $\text{Nb}_2\text{O}_5$  (99.9% Alfa Aesar) (total weight  $\sim 8$  g) and 50 agate balls with diameters of 10 mm were placed in an agate bowl (99.9%  $\text{SiO}_2$ ) with a maximum volume of 250 ml. 120 ml of ethanol (99.8%, Fluka) was added as a milling medium to prevent excessive abrasion. The mixture was milled using a planetary ball mill (Model Pulverisette 4 vario-Planetary mill) at different speeds (700, 1000, and 1400 rpm) for one hour in order to determine the optimum milling speed. The mixture was then dried at  $80^\circ\text{C}$  to evaporate the ethanol. For the conventional solid-state method, however, 3.0–4.0 g of the mixture of the required reagents were weighed and mixed manually using an agate mortar and pestle. Heat treatments with different temperatures and durations were carried out to ensure the formation of single-phase materials.

The samples were characterized via X-ray diffraction analysis (XRD) (Shimadzu diffractometer XRD 6000,  $\text{CuK}_\alpha$  radiation) in the  $2\theta$  range from  $10^\circ$ – $60^\circ$  at  $2^\circ \text{min}^{-1}$ . A chekcell refinement program was used to obtain the lattice parameters of the structure. The thermal events of samples were studied from room temperature to  $800^\circ\text{C}$  on heating and cooling cycles with a heating rate of  $10^\circ\text{C min}^{-1}$  by DTA (Perkin-Elmer instrument with model DTA 7).

The electrical properties were determined by AC impedance spectroscopy using a Hewlett Packard Impedance Analyzer, HP4192A, in the frequency range of 5–13 MHz. Measurements were made from  $200^\circ\text{C}$  to  $850^\circ\text{C}$  in incremental steps of  $50^\circ\text{C}$  on a heating cycle with a 30 min equilibration time.

## 3. RESULTS AND DISCUSSION

### 3.1 XRD Analysis

Figure 1 shows the phase evolution of  $\text{Bi}_3\text{NbO}_7$  synthesized by a mechanochemical process with a milling speed of 1000 rpm for one hour. From the results obtained, the mixture produced after milling one hour without any heat treatment consists of raw materials that are  $\text{Bi}_2\text{O}_3$  and  $\text{Nb}_2\text{O}_5$ , indicating that no reaction has occurred at this stage. After heating the precursor at  $600^\circ\text{C}$  for 24 h and  $650^\circ\text{C}$  for 72 h, traces of starting materials still remained, indicating that the reaction was not complete. A single-phase  $\text{Bi}_3\text{NbO}_7$  was successfully obtained after the ball-milled precursor was heated at  $700^\circ\text{C}$  for 24 h. The

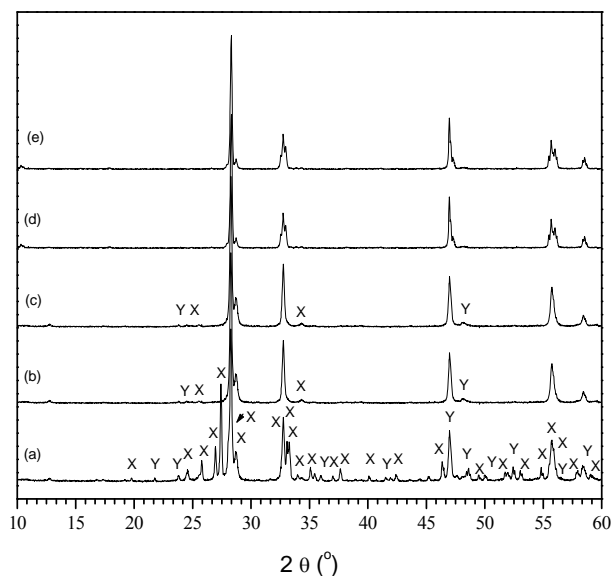


Figure 1: Phase evolution of  $\text{Bi}_3\text{NbO}_7$  synthesized via the mechanochemical method (1000 rpm for one hour) with synthesis temperature (X =  $\text{Bi}_2\text{O}_3$ , Y =  $\text{Nb}_2\text{O}_5$ ): (a) without heat treatment; (b)  $600^\circ\text{C}$  for 24 h; (c)  $650^\circ\text{C}$  for 48 h; (d)  $700^\circ\text{C}$  for 24 h; (e)  $800^\circ\text{C}$  for 24 h.

conventional solid-state method requires a higher temperature ( $800^\circ\text{C}$ ) and 24 h to obtain a pure phase compound. This may be due to the ball-milled method, which can result in a better mixing of chemicals and therefore can speed up the reaction rate and reduce the synthesis temperature.

The XRD patterns of  $\text{Bi}_x\text{NbO}_8$  ( $2 \leq x \leq 7$ ) solid solutions are shown in Figure 2. Solid solutions with a single-phase were formed in the range of  $2.5 \leq x \leq 6$ . There is an expected small shift in the  $2\theta$  at  $\sim 28.20^\circ$  due to the increasing Bi content that can change the atomic arrangement in the structure, resulting in a shift in the d-spacing.<sup>11</sup> Refinements were performed using a chekcell program with a lattice of  $\text{Bi}_3\text{NbO}_7$  reported by Ling and Johnson as starting values.<sup>11</sup> All of the peaks in the XRD patterns of these materials can be fully indexed in a tetragonal system with a space group of  $I4m2$ .

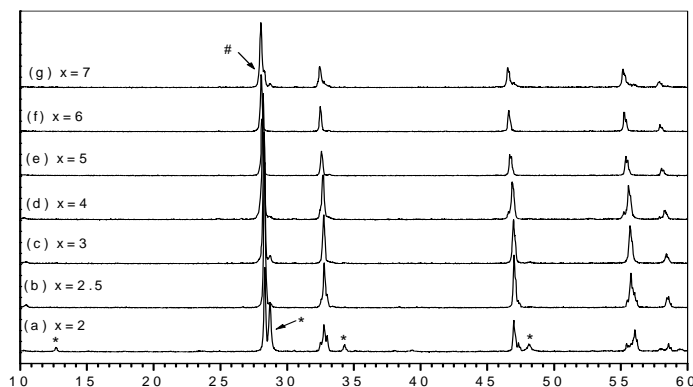


Figure 2: XRD patterns of  $\text{Bi}_x\text{NbO}_8$  ( $2 \leq x \leq 7$ ) prepared via the mechanochemical method. (# =  $\text{BiNbO}_4$ ; \* =  $\text{Bi}_5\text{Nb}_3\text{O}_{15}$ )

$\text{Bi}_2\text{NbO}_{5.5}$  ( $x=2$ ), a mixed-phase that consists of  $\text{Bi}_3\text{NbO}_7$  and  $\text{Bi}_5\text{Nb}_3\text{O}_{15}$ , was obtained. The presence of the  $\text{Bi}_5\text{Nb}_3\text{O}_{15}$  phase was indicated by unindexed peaks at  $2\theta = 12.68^\circ$  and  $48.11^\circ$ . For values of  $x$  larger than 6, a peak around  $27.94^\circ$  was obtained corresponding to  $\text{BiNbO}_4$ , which is determined by comparing the XRD pattern of  $\text{Bi}_7\text{NbO}_{13}$  to that of  $\text{BiNbO}_4$  reported in ICDD card number: 00-016-0486 indicating the presence of a mixed-phase. The intensity of this peak did not change, even after heat treatment at  $900^\circ\text{C}$  for 72 h.

### 3.2 Thermal Analyses

DTA measurements were carried out on all of the solid solutions to investigate the thermal events. Figure 3 shows the DTA thermograms of materials in  $\text{Bi}_x\text{NbO}_8$  ( $2.5 \leq x \leq 6$ ) solid solutions at a heating and cooling rate of  $10^\circ\text{C min}^{-1}$ . From the results, no thermal changes and phase transitions were observed. Straight lines observed in the TGA thermograms for samples in the solid solutions showed that there was no weight loss when samples were heated to  $800^\circ\text{C}$ . This indicates that these materials were thermally stable.

### 3.3 Conductivity Measurement

The impedance ( $Z^*$ ) complex plane ( $Z''$  vs.  $Z'$ ) plots measured at three different temperatures ( $300^\circ\text{C}$ ,  $550^\circ\text{C}$ , and  $800^\circ\text{C}$ ) for  $\text{Bi}_3\text{NbO}_7$  synthesized via the mechanochemical method are presented in Figure 4. An equivalent circuit consisting of two parallel RC elements connected in series as shown in

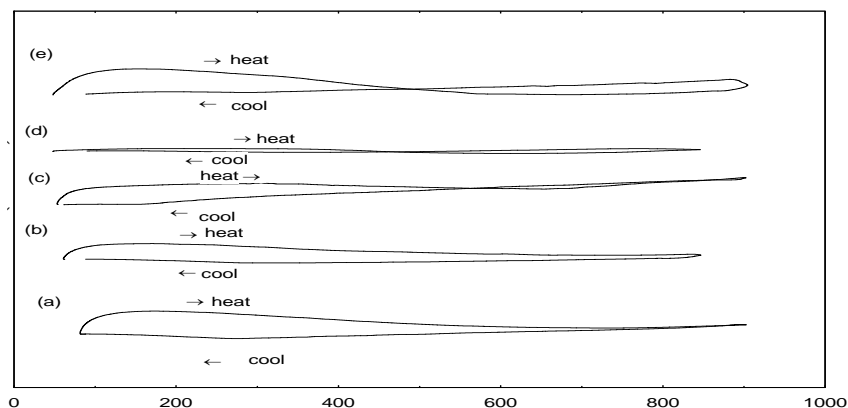


Figure 3: DTA thermograms: (a)  $\text{Bi}_{2.5}\text{NbO}_{6.25}$ ; (b)  $\text{Bi}_3\text{NbO}_7$ ; (c)  $\text{Bi}_4\text{NbO}_{8.5}$ ; (d)  $\text{Bi}_5\text{NbO}_{10}$ ; (e)  $\text{Bi}_6\text{NbO}_{11.5}$  synthesized by the mechanochemical method.

Figure 4(a) was used to interpret the  $Z^*$  plots. One RC element,  $R_bC_b$ , models the electrical response of the bulk, whereas the other,  $R_{gb}C_{gb}$ , models the grain boundary response. The overall sample impedance is the summation of  $R_b$  and  $R_{gb}$ . The complex plane plot of  $\text{Bi}_3\text{NbO}_7$  measured at  $300^\circ\text{C}$  is shown in Figure 4(a). Generally, the high frequency arc has an associated capacitance of around  $10^{-12} \text{ Fcm}^{-1}$ , which is a typical value for the bulk (intragranular) capacitance of a sample. Figure 4(a) has a capacitance of this order and, thus, this contribution was interpreted as resulting from the bulk resistance of the sample.

At  $550^\circ\text{C}$  a small, low frequency spike was observed as illustrated in Figure 4(b), which is characteristic of an ionic polarization phenomenon at the blocking electrode, which is known as a Warburg-response. At  $800^\circ\text{C}$ , the diffusion of oxygen ions through the entire thickness of the electrode was seen in the collapse of the spike into a semicircular arc [Fig. 4(c)], supporting the idea that the conducting species were predominantly oxide ions. Similar impedance data were observed for the solid solutions.

Combined spectroscopic plots of the imaginary components of the impedance,  $Z''$ , and the electric modulus,  $M''$ , can be used as a general method for probing the electrical homogeneity for ceramics. For an ideal Debye response representing bulk properties, the frequency maxima of  $Z''$  and  $M''$  peaks should be coincident and the half-height peak widths should be 1.14 decades on a log  $f$  scale for a homogenous material.<sup>14</sup> The combined spectroscopic of  $M''$  and  $Z''$  versus the log  $f$  for  $\text{Bi}_3\text{NbO}_7$  (Fig. 5) showed two non-overlapping peaks at

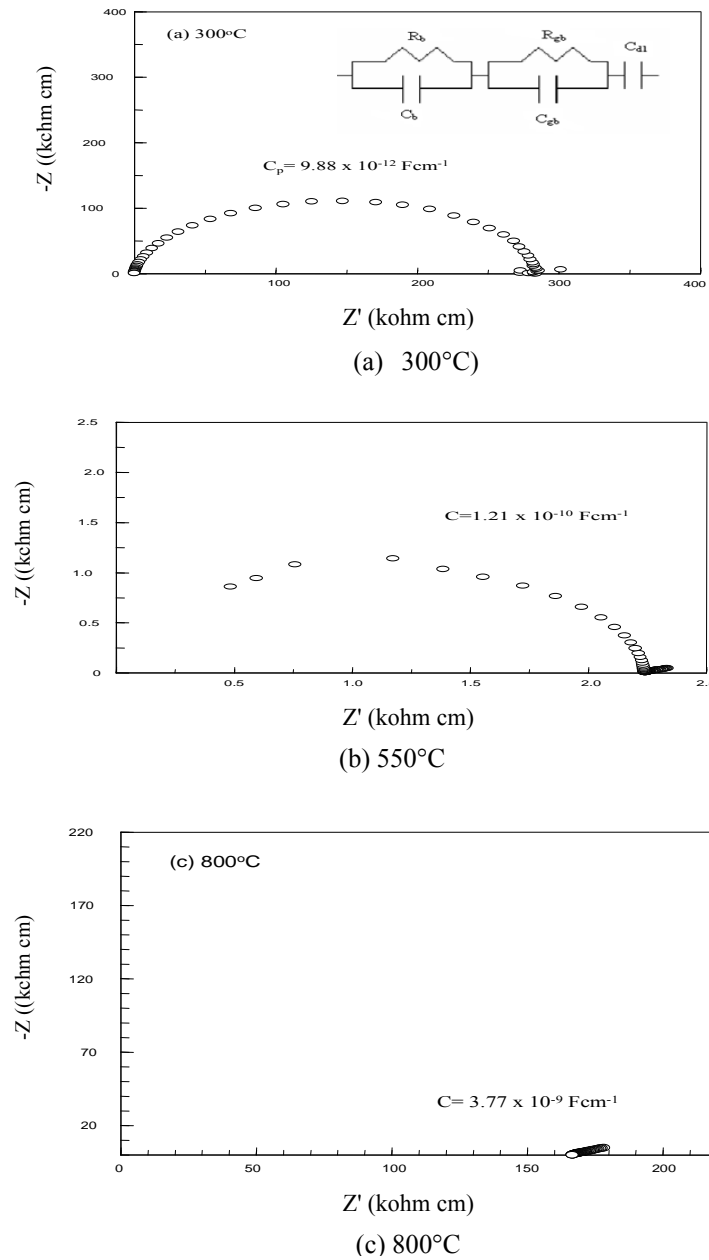


Figure 4: Complex impedance plane plots for  $\text{Bi}_3\text{NbO}_7$  at (a) 300°C, (b) 550°C, and (c) 800°C.

300°C. The half-height peak width of the  $M''$  peak has a value of around 1.57 on the  $\log f$  scale and this indicates that the conductivity measured is not that of the bulk alone and the material may not be homogenous.

Conductivity measurements were carried out on single-phase materials. Conductivity values were extracted from the AC impedance data. These materials showed reproducible conductivity in the heating and cooling cycles. Figure 6 shows the Arrhenius plots of  $\text{Bi}_x\text{NbO}_8$  ( $2.5 \leq x \leq 6$ ) during the first cooling cycle. The conductivity values range from  $10^{-7}$  to  $10^{-2} \text{ ohm}^{-1}\text{cm}^{-1}$  between 250°C and 800°C. Among the materials prepared,  $\text{Bi}_6\text{NbO}_{11.5}$  has the highest conductivity ( $5.0 \times 10^{-5} \text{ ohm}^{-1}\text{cm}^{-1}$  at 300°C). Table 1 lists the conductivity values at 300°C and 600°C, and the  $E_a$  values for all of the samples of  $\text{Bi}_x\text{NbO}_8$  ( $2.5 \leq x \leq 6$ ). The Arrhenius plot of YSZ is included for comparison purposes.<sup>15</sup> In general, at 300°C, the conductivity decreased in order of:

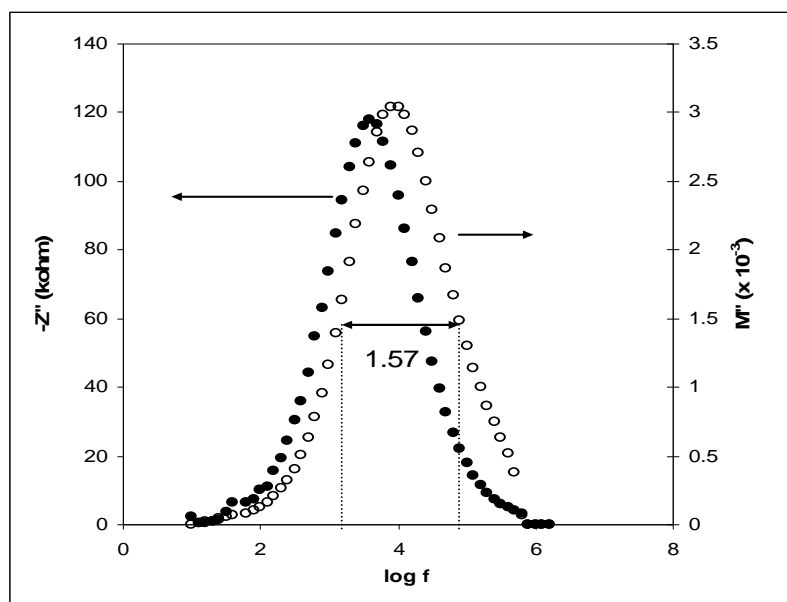


Figure 5: A combined  $Z''$  and  $M''$  spectroscopic plot for  $\text{Bi}_3\text{NbO}_7$  at 300°C.

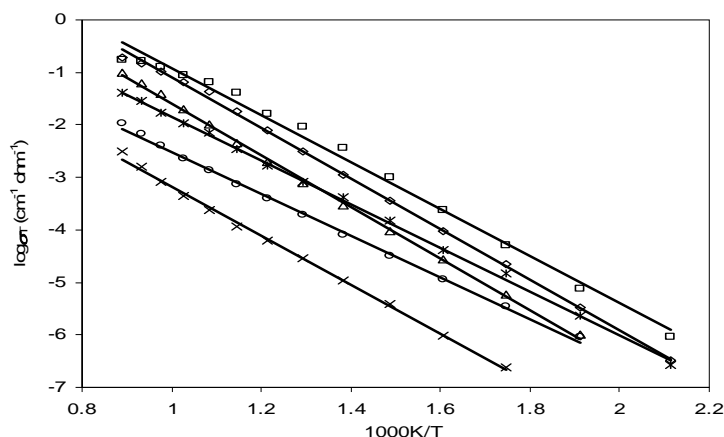


Figure 6: Arrhenius plots of  $\text{Bi}_x\text{NbO}_8$  ( $2.5 \leq x \leq 6$ ) synthesized via the mechanochemical method. ( $x = \text{Bi}_{2.5}\text{NbO}_{6.25}$ ;  $\circ = \text{Bi}_3\text{NbO}_7$ ;  $\Delta = \text{Bi}_4\text{NbO}_{8.5}$ ;  $\diamond = \text{Bi}_5\text{NbO}_{10}$ ;  $\square = \text{Bi}_6\text{NbO}_{11.5}$ ;  $*$  = YSZ)

Table 1: Conductivities ( $\sigma_{300}$  and  $\sigma_{600}$ ) and  $E_a$  of  $\text{Bi}_x\text{NbO}_8$  ( $2.5 \leq x \leq 6$ ) synthesized via the mechanochemical method.

x	$\sigma_{300} \times 10^{-6} \text{ ohm}^{-1}\text{cm}^{-1}$	$\sigma_{600} \times 10^{-3} \text{ ohm}^{-1}\text{cm}^{-1}$	$E_a$ (eV)
2.5	0.24	0.12	0.93
3	3.57	0.75	0.79
4	5.88	4.57	0.97
5	21.5	16.9	0.95
6	50.0	46.7	0.89
YSZ	15.00	3.53	0.82

Figure 7 shows the comparison of the Arrhenius plots of  $\text{Bi}_3\text{NbO}_7$  synthesized by the solid-state and mechanochemical methods. Based on the results, there is no significant difference in the conductivities between the two samples synthesized via the two different methods. The slopes of the plots are determined to be 0.79 eV for the compound prepared via the mechanochemical method and 0.83 eV for the solid-state method, respectively. The sample prepared by the mechanochemical method showed a lower  $E_a$ , which appears to increase the mobility of free charge carriers compared to the sample prepared by the solid-state method over the entire investigated temperature range.

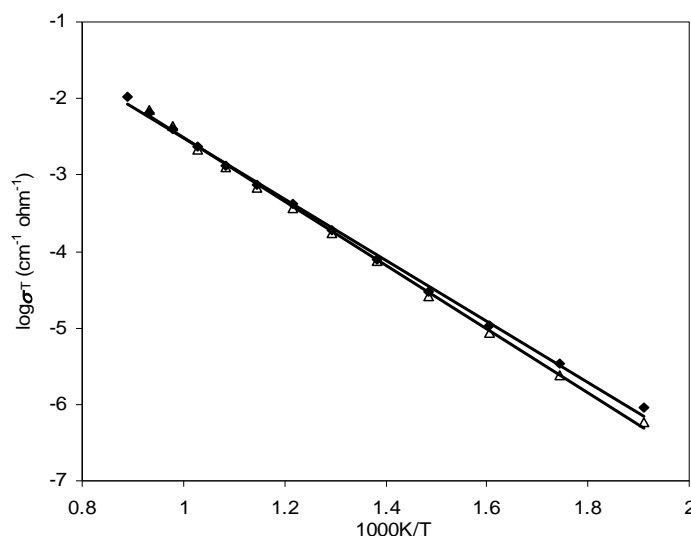


Figure 7: Arrhenius plots of  $\text{Bi}_3\text{NbO}_7$  synthesized via the solid-state ( $\Delta$ ) and mechanochemical ( $\blacklozenge$ ) methods.

#### 4. CONCLUSION

Materials in  $\text{Bi}_2\text{O}_3$ - $\text{Nb}_2\text{O}_5$  binary systems have been successfully synthesized via a mechanochemical method at lower synthesis temperatures (milled at 1000 rpm for one hour followed by heating at  $700^\circ\text{C}$  for 24 h) than the solid-state method, which required a higher temperature ( $800^\circ\text{C}$  for 24 h). The ball milled method may have produced better mixing of the chemicals, thereby increasing the reaction rate and reducing the synthesis temperature. A series of solid solutions  $\text{Bi}_x\text{NbO}_8$  was obtained at  $2.5 \leq x \leq 6$ . Electrical measurements indicated that there was no significant difference in the conductivities of the  $\text{Bi}_3\text{NbO}_7$  synthesized by the two different methods. The sample prepared using the mechanochemical method showed a relatively lower  $E_a$ , which appears to increase the mobility of free charge carriers compared with the sample prepared by the solid-state method.

#### 5. ACKNOWLEDGMENTS

The authors are grateful for financial support given by the Ministry of Science, Technology, and Innovation (MOSTI) via the Science Fund and National Science Fellowship (NSF) scholarship for S.N. Ng.

## 6. REFERENCES

1. Takahashi, T. & Iwahara, H. (1978). Oxide ion conductors based on bismuthsesquioxide. *Mater. Res. Bull.*, 13, 1447–1453.
2. Sammes, N.M., Tompsett, G.A., Näfe, H. & Aldinger, F. (1998). Bismuth based oxide electrolytes-structure and ionic conductivity. *J. Eur. Ceram. Soc.*, 19, 1801–1826.
3. Biovin, J.C. (2001). Structural and electrochemical feature of fast oxide ion conductors. *Int. J. Inorg. Mater.*, 3, 1261–1266.
4. Fruth, V., Ianculescu, A., Berger, D., Preda, S. & Voicu, G. (2006). Synthesis, structure and properties of doped  $\text{Bi}_2\text{O}_3$ . *J. Eur. Ceram. Soc.*, 26, 3011–3016.
5. Harwig, H.A. & Gerrards, A.G. (1978). Electrical properties of the  $\alpha$ ,  $\beta$ ,  $\gamma$  and  $\delta$  phases of bismuth sesquioxide. *J. Solid State Chem.*, 26, 265–274.
6. Zhou, W., Jefferson, D.A. & Thomas, J.M. (1987). A new structure type in the  $\text{Bi}_2\text{O}_3$ - $\text{Nb}_2\text{O}_5$  system. *J. Solid State Chem.*, 70, 129–136.
7. Shuk, P., Wiemhöfer, H.D., Guth, U., Göpel, W. & Greenblatt, M. (1996). Oxide ion conducting solid electrolytes based on  $\text{Bi}_2\text{O}_3$ . *Solid State Ionics*, 89, 179–196.
8. Castro, A., Aguado, E., Rojo, J.M., Herrero, P., Enjalbert, R. & Galy, J. (1997). The new oxygen-deficient fluorite  $\text{Bi}_3\text{NbO}_7$ : Synthesis electrical behavior and structural approach. *Mater. Res. Bull.*, 33(1), 31–41.
9. Lazarraga, M.G., Amarilla, J.M., Rojas, R.M. & Rojo, J.M. (2005). The cubic  $\text{Bi}_{1.76}\text{U}_{0.12}\text{La}_{0.12}\text{O}_{3.18}$  mixed oxide: Synthesis, structural characterization, thermal stability and electrical properties. *Solid State Ionics*, 89, 179–196.
10. Wang, X.P., Corbel, G., Kodjikian, S., Fang, Q.F. & Lacorre, P. (2006). Isothermal kinetic of phase transformation and mixed electrical conductivity in  $\text{Bi}_3\text{NbO}_7$ . *J. Solid State Chem.*, 179, 3338–3346.
11. Ling, C.D. & Johnson, M. (2004). Modelling, refinement and analysis of the “type III”  $\delta$ - $\text{Bi}_2\text{O}_3$ -related superstructure in the  $\text{Bi}_2\text{O}_3$ - $\text{Nb}_2\text{O}_5$  system. *J. Solid State Chem.*, 177, 1838–1846.
12. Kong, L.B., Ma, J., Zhu, W. & Tan, O.K. (2001). Preparation of  $\text{Bi}_4\text{Ti}_3\text{O}_{12}$  ceramics via a high-energy ball milling process. *Mater. Lett.*, 51, 108–114.
13. Moreno, K.J., Fuentes, A.F., García-Barriocanal, J., León, C. & Santanmaría, J. (2005). Mechanochemical synthesis and ionic conductivity in  $\text{Gd}(\text{Sn}_{1-y}\text{Zr}_y)_2\text{O}_7$  ( $0 \leq y \leq 1$ ) solid solution. *J. Solid State Chem.*, 178, 3771–3778.

14. Sinclair, D.C., Morrison, F.D. & West, A.R. (2000). Application of combined impedance and electrical modulus spectroscopy to characterize electroceramics. *Int. Ceram.*, 2, 33–38.
15. West, A.R. (1999). *Basic solid state chemistry*, 2<sup>nd</sup> ed. Chichester: John and Sons.